

# Extrinsic dislocation loop behavior in silicon with a thermally grown silicon nitride film

S. B. Herner,<sup>a)</sup> V. Krishnamoorthy, and K. S. Jones

Department of Materials Science and Engineering, University of Florida, Gainesville, Florida 32611

T. K. Mogi<sup>b)</sup> and M. O. Thompson

Department of Materials Science and Engineering, Cornell University, Ithaca, New York 14853

H.-J. Gossmann

Bell Laboratories, Lucent Technologies, Murray Hill, New Jersey 07974

(Received 6 September 1996; accepted for publication 24 February 1997)

The effect of a thermally grown silicon nitride ( $\text{SiN}_x$ ) film on end-of-range extrinsic dislocation loops in a silicon substrate was investigated by transmission electron microscopy. A layer of extrinsic dislocation loops was formed by annealing a Si wafer amorphized by a  $\text{Ge}^+$  ion implant. A nitride film was grown on the Si by further annealing in ammonia ( $\text{NH}_3$ ) at 810 and 910 °C for 30–180 min. Wafers with a loop layer were also annealed in argon (Ar) at the same conditions as the  $\text{NH}_3$ -annealed wafers to determine loop behavior in an inert environment. Samples annealed in  $\text{NH}_3$  had a significant decrease in the net number of interstitials bound by the loops, while those annealed in Ar showed no change. The results are explained by a supersaturation of vacancies caused by the presence of the nitride film, resulting in loop dissolution. By integrating the measured vacancy flux over the distance from the nitride/Si interface to the loop layer, we extract an estimate for the relative supersaturation of vacancies at 910 °C,  $C_V/C_V^* \sim 4$ , where  $C_V$  is the concentration of vacancies and the asterisk denotes equilibrium. We rule out interstitial undersaturation-induced loop dissolution based on loop stability with temperature and oxidation-enhanced loop growth calculations. A comparison with estimated  $C_V/C_V^*$  values from a previous report using the same processing equipment and parameters but monitoring the change in Sb diffusivity with nitridation shows excellent agreement. © 1997 American Institute of Physics. [S0021-8979(97)01211-5]

## I. INTRODUCTION

As device dimensions in integrated circuits continue to decrease, there is a need to minimize the thermal budget that wafers are exposed to during processing. This need is driven, among other things, by the need to minimize dopant diffusion. Dopant diffusion in silicon (Si) is controlled by the concentration of native point defects, namely Si vacancies and self-interstitials.<sup>1</sup> It is therefore crucial to understand how the concentration of native point defects in Si changes with each processing step, and how point defects interact with extended defects and interfaces. In this report, we examine the behavior of preexisting extrinsic dislocation loops in Si samples annealed in either ammonia ( $\text{NH}_3$ ) or argon (Ar) at 810 or 910 °C. Samples annealed in  $\text{NH}_3$  form a silicon nitride ( $\text{SiN}_x$ ) film. End-of-range (EOR) dislocation loops are typically observed in ion implanted Si at doses above the amorphization threshold.<sup>2</sup> Through observation of loop behavior, we can gain insight as to how the concentration of point defects changes with a particular processing step.

It has been established that the growth of a thermal  $\text{SiN}_x$  film results in a vacancy supersaturation and interstitial undersaturation in the underlying Si.<sup>3–5</sup> In a previous study, Mogi *et al.*<sup>5</sup> showed that anneal of Si in  $\text{NH}_3$  resulted in  $C_V/C_V^* \sim 4$  and  $C_I/C_I^* \sim 0.2$  at a temperature of 910 °C,

where  $C_V$  denotes the volume concentration of vacancies,  $C_I$  that of interstitials, and the asterisk denotes equilibrium. These values were determined by measuring the diffusivity of antimony (Sb) and boron (B) in Si doping superlattices (DSLs). Antimony has been shown to diffuse by a vacancy-assisted mechanism, while boron diffuses primarily by an interstitial(cy)-assisted mechanism.<sup>3,6</sup> The diffusivity of Sb and B is therefore proportional to the concentration of vacancies and self-interstitials, respectively, and hence concentra-

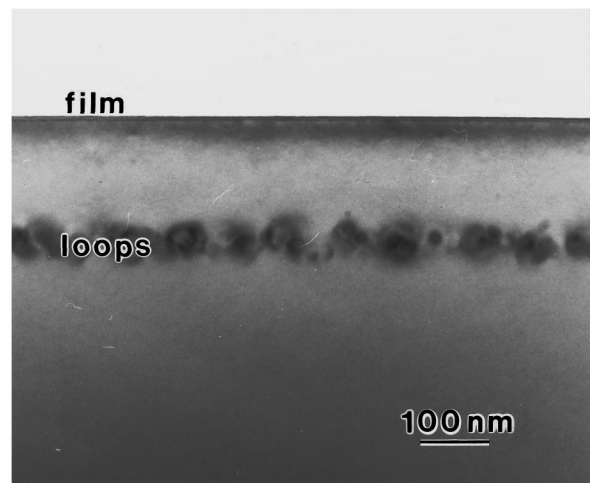


FIG. 1. Cross-sectional TEM micrograph of the sample annealed at 910 °C for 180 min in  $\text{NH}_3$ .

<sup>a)</sup>Present address: Bell Laboratories, Lucent Technologies, Murray Hill, NJ 07974. Electronic mail: bherner@physics.bell-labs.com

<sup>b)</sup>Present address: McKinsey and Co., Stamford, CT.

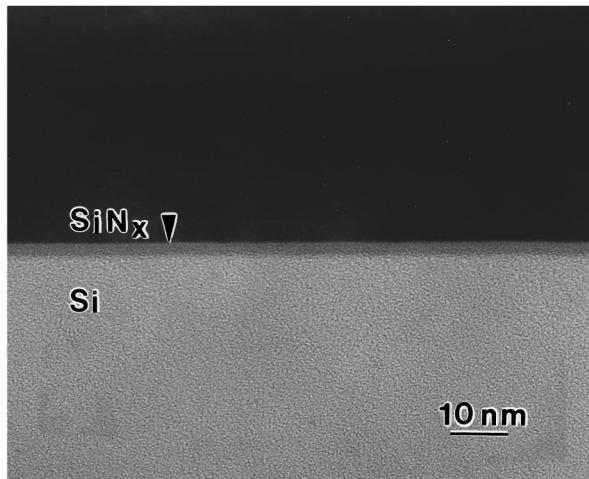


FIG. 2. High magnification (800 000 $\times$ ) cross-sectional TEM micrograph of the SiN<sub>x</sub> film on the sample annealed at 910 °C for 180 min. in NH<sub>3</sub>.

tion depth profiles of self-interstitials and vacancies are obtained. The primary quantity measured in dopant marker experiments is the relative supersaturation or undersaturation of point defects. In principle, the act of detection requires point defect-dopant binding energies to be taken into account. While it has been shown in doping superlattices of B that the act of detection by itself does not perturb the point defect concentration,<sup>7</sup> the dislocation loop method eliminates the need to even consider this.

The primary quantity measured by the loops is the *flux* of point defects introduced by a processing step such as thin film growth on the substrate surface. However, one must account for the fraction of loop dissolution/growth caused by a change in the concentration of both kinds of point defects. For example, loop dissolution can be attributed to vacancy supersaturation or interstitial undersaturation. While this problem can be ignored for studies in which the change in concentration of one point defect far exceeds that in the other, as occurs in ion implantation,<sup>8</sup> it cannot be ignored for

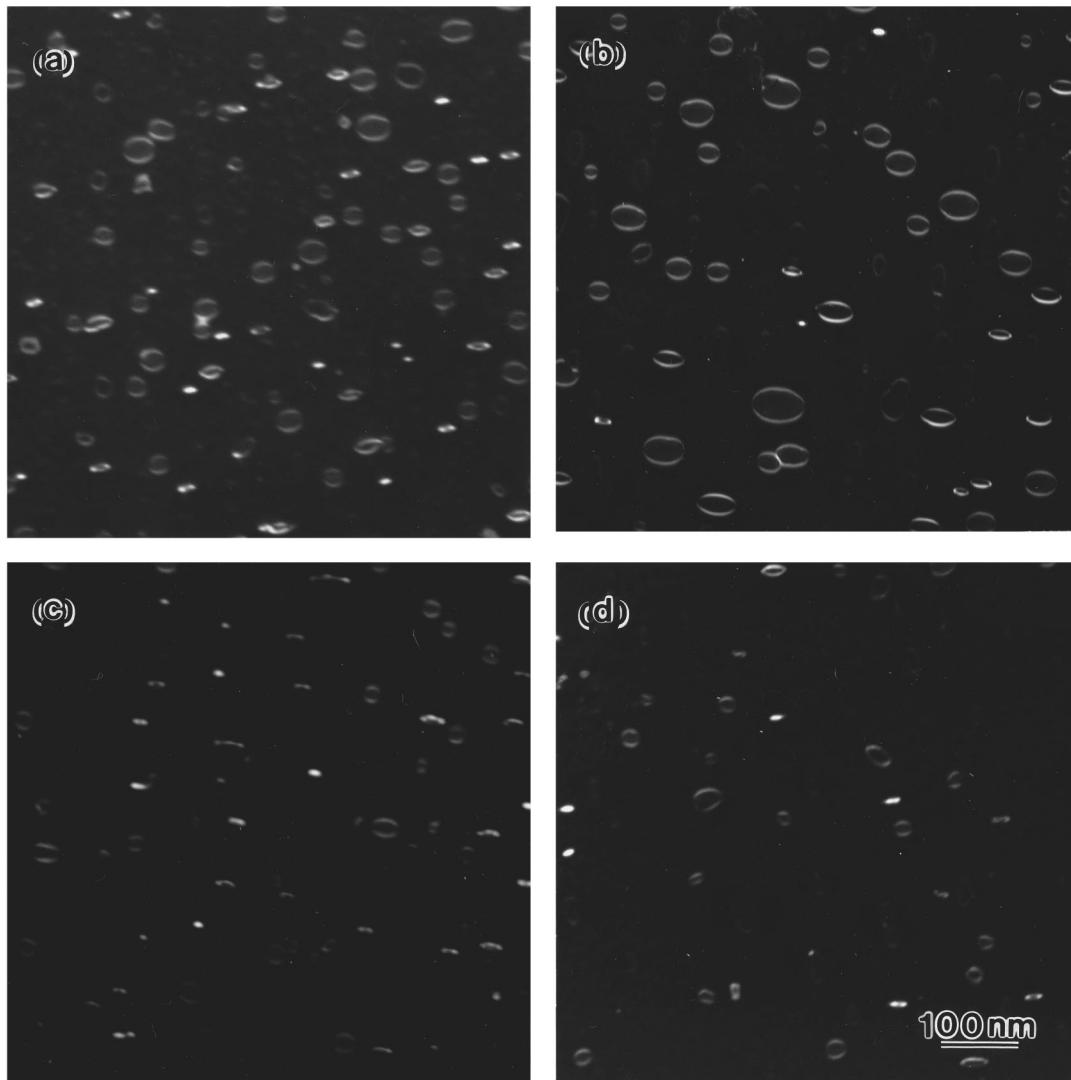


FIG. 3. Plan view TEM micrographs of the samples annealed at 910 °C for (a) 30 min in Ar; (b) 180 min in Ar; (c) 30 min in NH<sub>3</sub>, and (d) 180 min in NH<sub>3</sub>.

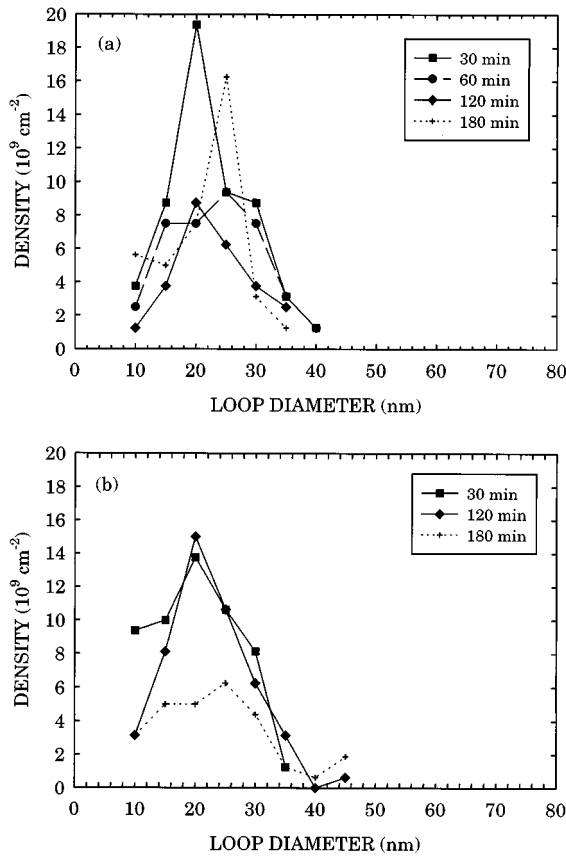


FIG. 4. Size distributions of the loops in samples annealed in Ar at (a) 810 °C and (b) 910 °C.

studies in which the relative changes in the point defect concentrations are smaller and similar in magnitude, as is the case here.

## II. EXPERIMENT

A Czochralski-grown *p*-type Si wafer ( $\rho < 100 \Omega \text{ cm}$ ) was implanted with 140 keV  $\text{Ge}^+$  ions to a dose of  $1 \times 10^{15} \text{ cm}^{-2}$  in order to amorphize the Si. The beam current was kept below  $1 \mu\text{A cm}^{-2}$  to limit possible dose-rate heating effects. The wafer was annealed in flowing  $\text{N}_2$  (99.999% purity) at 800 °C for 60 min to recrystallize the amorphized region and form the EOR loops. Annealing under these conditions has been previously shown to return the point defect concentrations to equilibrium after the disturbance caused by ion implantation.<sup>8</sup> The annealed wafer was diced and cleaned by a dilute HF (1:20) dip prior to furnace entry. Half the samples were annealed in a quartz tube furnace with flowing  $\text{NH}_3$  (99.9995% purity) at one atmosphere, with 25 sccm gas flow at temperatures of 810 or 910 °C and times ranging from 30 to 180 min. The second set of samples were annealed in argon (99.95% purity) for the same times and temperatures, and were used as controls. Samples were examined in a JEOL 200CX transmission electron microscope (TEM) operating at 200 keV. Samples for plan view TEM (PTEM) were prepared by standard mechanical lapping and chemical etching methods. Cross-sectional TEM (XTEM)

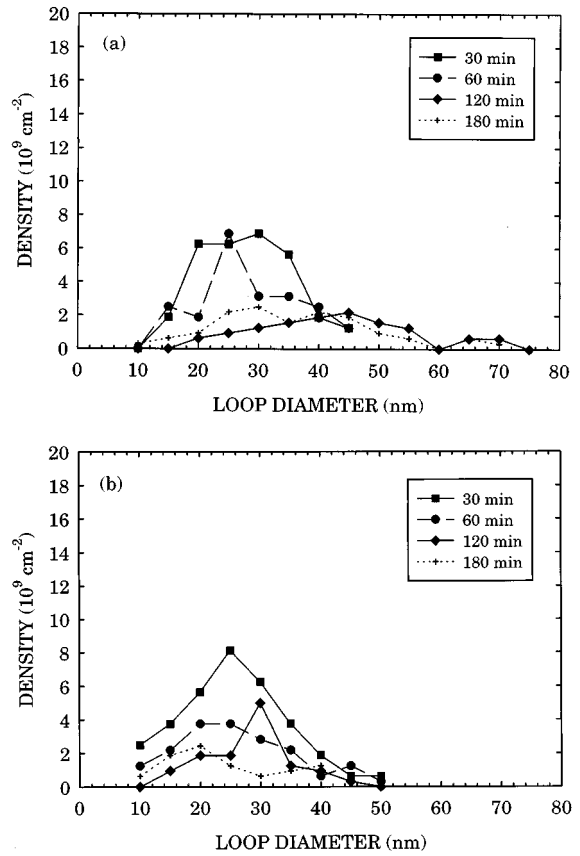


FIG. 5. Size distributions of the loops in samples annealed in  $\text{NH}_3$  at (a) 810 °C and (b) 910 °C.

samples were prepared by lapping and ion milling. Quantitative analysis of the dislocation loops was performed using weak beam dark field ( $g_{220}$ ) PTEM micrographs. All the loops were measured in a representative area of  $\sim 1 \mu\text{m}^2$  in each sample. Loop diameters were measured in increments of 5 nm from 10 to 70 nm by measuring the longest axis on each loop. The total number of loops of each size was multiplied by the area of that size loop and the area added to get the total area of the loops. Previous experiments have shown that the loops tend to lie on  $\{111\}$  planes.<sup>2,8</sup> The net density of Si interstitials bound by the loops in each sample was calculated by multiplying the area bound by the loops by  $1.6 \times 10^{15} \text{ cm}^{-2}$ . The details of the analysis, as well as the error measurement, have been described in greater detail by Listebarger *et al.* in Ref. 8.

## III. RESULTS AND DISCUSSION

A typical XTEM micrograph of the film and loop layer is shown in Fig. 1. The dislocation loop layer is approximately 160 nm below the surface and the layer is 30 nm wide. The thickness of the film was measured to be 4 nm from the sample annealed at 910 °C for 180 min (Fig. 2). This provides a maximum thickness of all films grown since it had the longest time and highest temperature anneal. Little variation of the thickness has been seen in samples annealed at 810 °C for the shorter times. This is in agreement with previous results on thermally grown nitride films.<sup>9</sup>

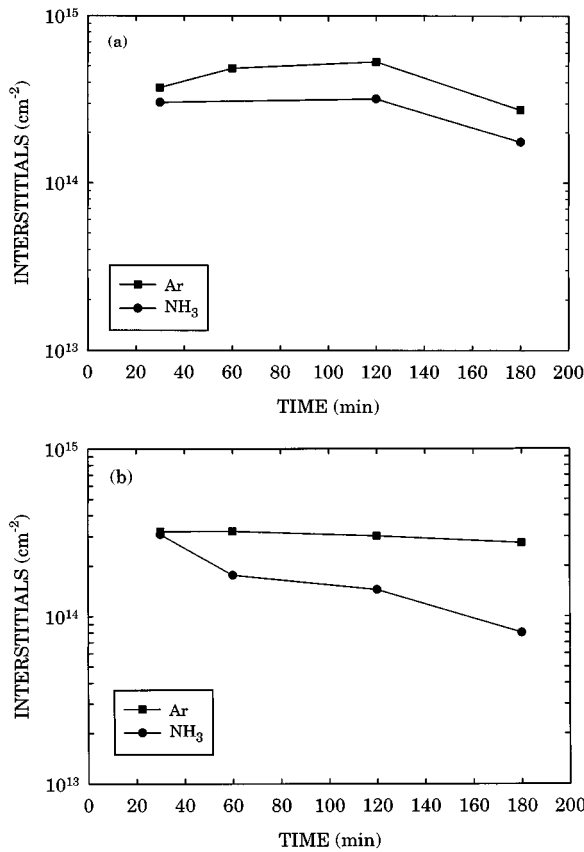


FIG. 6. Net density of interstitials bound by the loops in both sets of samples.

### A. Loop distributions

We divide the samples into those annealed in  $\text{NH}_3$  (nitrided) and those that are annealed in Ar (controls). Representative PTEM micrographs of dislocation loop evolution during annealing are shown in Fig. 3. From the data, the loops show an increase in average size and a decrease in density in both sets of samples with increased anneal time and temperature. The size distributions of the loops are plotted in Figs. 4 and 5. The loops in the 810 °C Ar-annealed samples do not show a significant coarsening [Fig. 4(a)]. The relatively small shift in the peak density of loop sizes from 20 to 25 nm in the 30 to 180 min anneal, respectively, is indicative of this. The loops in the 910 °C Ar-annealed samples show a much more distinctive shift to the larger sizes with annealing. While the shift to larger loop sizes is subtle, the number of interstitials bound in the larger loops increases rapidly due to the  $r^2$  dependence, where  $r$  is the radius of the loop. The reduction in the amount of loops with the most common size diameter from the 810 °C anneal [Figs. 4(a)–5(a)] to the 910 °C anneal [Figs. 4(b)–5(b)] indicates nonthermal dissolution of the loops is occurring in the samples annealed in  $\text{NH}_3$ . While the loop density at the peak of the distribution decreases with time, the loop diameter corresponding to the peak increases.

Little thermal dissolution of the loops is occurring in the Ar-annealed samples, as observed by the constancy of the net interstitials bound by the loops (Fig. 6). The peak height

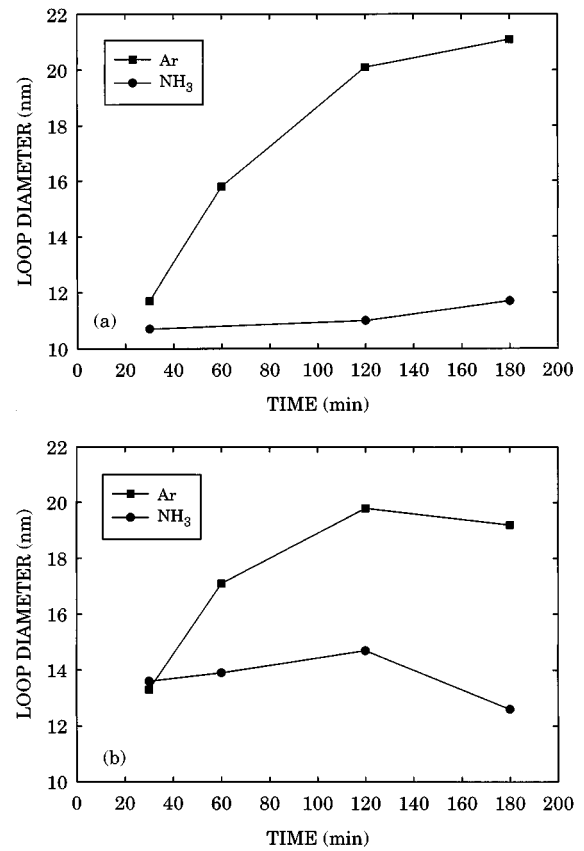


FIG. 7. Weighted average loop radii normalized by the area of each loop size in samples annealed at (a) 810 °C and (b) 910 °C.

shows large statistical error associated with it and no conclusions can be drawn from it. However, the integrated area under the peak shows unequivocally that thermal dissolution is not occurring in the control samples. Also, it can be concluded that the loops are in a coarsening and not growth regime. The nitrided samples show a net decrease in interstitials bound by the loops. A comparison of the loop distribution between Ar- and  $\text{NH}_3$ -annealed samples shows that nitridation results in loop dissolution. Loop coarsening in the nitrided samples must then compete with nonthermal loop dissolution. In order to estimate the extent of coarsening, the weighted average loop radii (normalized to the density of interstitials bound by a particular size loop) are shown in Figs. 7(a) and 7(b). The weighted average loop radii is calculated by

$$r_{\text{weighted}} = \left( \frac{\sum_i n_i r_i^2}{\sum_i n_i} \right)^{1/2}, \quad (1)$$

where  $n_i$  is the area density of loops with a radius  $r_i$ . This method normalizes the radius by the amount of interstitials bound by the loops of each size. The figures show the loops in the control samples annealed in Ar coarsen to a greater extent than the loops in the samples annealed in  $\text{NH}_3$  at both anneal temperatures, which again demonstrates that loop dissolution in the nitrided samples dominates over coarsening.

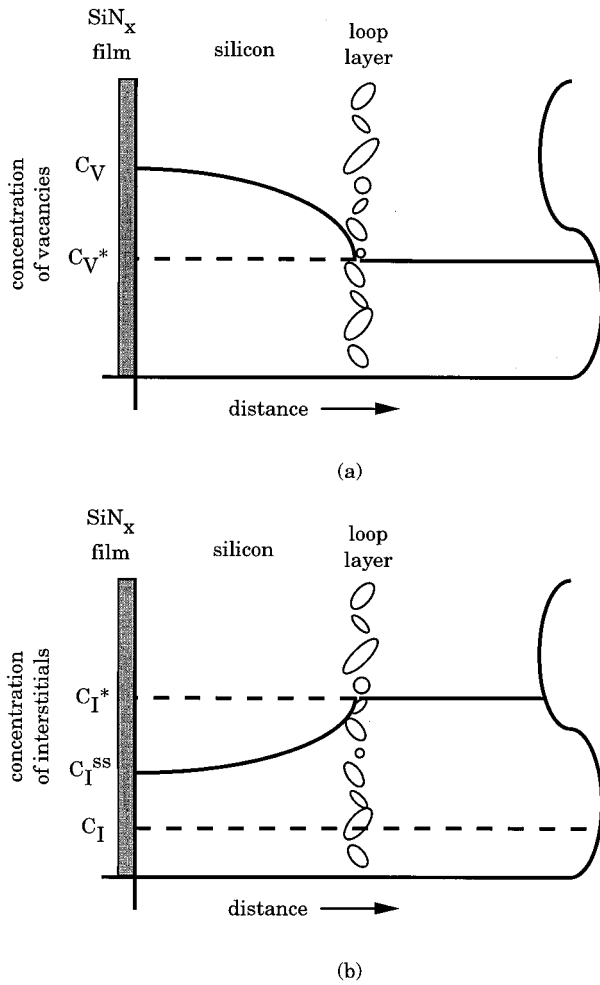


FIG. 8. Schematic of concentration depth profiles of (a) vacancies and (b) interstitials.

The dissolution can be explained by vacancy supersaturation and/or interstitial undersaturation caused by the presence of the nitride film.

## B. Point defect–loop interaction

Extrinsic dislocation loop dissolution via native point defects can occur by a vacancy supersaturation and/or interstitial undersaturation.<sup>10</sup> We examine each case individually.

### 1. Vacancy supersaturation

By assuming that a flux,  $\Phi$ , of vacancies from the  $\text{SiN}_x$  film to the bulk is completely captured and annihilated by the loops, and that all loop dissolution is due to loop–vacancy interaction, one can integrate the flux over the distance via

$$\int_0^d \Phi dx = (C_V - C_V^*) D_V, \quad (2)$$

where  $\Phi$  is the number of interstitials lost by the loops per unit area and time,  $d$  is the distance from the interface to the loop layer, and  $D_V$  is the diffusivity of vacancies. This calculation assumes a constant flux over time and a negligible loss of vacancies from free interstitial (I)–free vacancy (V) recombination. The values for  $\Phi$  are then

TABLE I. Values used to calculate vacancy supersaturation-induced loop dissolution.

Parameter	Value at 910 °C
$\int_0^d \Phi dx$ (this study)	$(6.4 \pm 1.7) \times 10^5 \left( \frac{\text{vac}}{\text{cm s}} \right)$
$C_V^* D_V$ (Ref. 6)	$2.0 \times 10^5 \left( \frac{\text{vac}}{\text{cm s}} \right)$
$\frac{C_V}{C_V^*}$ (Ref. 5 after 60 min anneal)	$3.8 \pm 1.4$
$\frac{C_V}{C_V^*}$ (this study after 60 min anneal)	$4.2 \pm 0.9$

$$\Phi = \frac{\text{interstitials}_{\text{loops}}^{\text{Ar}} - \text{interstitials}_{\text{loops}}^{\text{NH}_3}}{\text{time}}. \quad (3)$$

A schematic of the vacancy profile is shown in Fig. 8(a). The time averaged integrated  $\Phi$  value for a 60 min  $\text{NH}_3$  anneal is shown in Table I. We found little change in  $\Phi$  with time at 910 °C, in agreement with the results of Mogi *et al.*,<sup>5</sup> who did not find a significant change in the enhancement of  $D_{Sb}$  with continued annealing at 910 °C.

We can compare the loop results to the previous study by Mogi *et al.*<sup>5</sup> using a  $C_V^* D_V$  value from the estimate by Tan and Gösele.<sup>6</sup> The analysis is limited to the 910 °C annealed samples because they are the only directly comparable data set. Using the integrated flux values and the  $C_V^* D_V$  estimate, we extract a value for  $C_V/C_V^*$  at 910 °C (Table I). The values from the two studies show excellent agreement. Since the methods used to estimate vacancy supersaturations in the two studies were based on completely different physical phenomena, we can be confident of the values extracted. This is useful in light of the fact that reported literature values for point defect parameters, e.g., interstitial diffusivities, extend over many orders of magnitude.<sup>11</sup> Hence we conclude that loop dissolution can be explained by a vacancy supersaturation on the order of  $C_V/C_V^* \sim 4$  in Si annealed in  $\text{NH}_3$  at 910 °C.

### 2. Interstitial undersaturation

The situation is more complex for interstitial undersaturation-induced loop dissolution. In this case, interstitials are leaving the loops to replenish an undersaturation in the area between the loops and the  $\text{SiN}_x/\text{Si}$  interface, so the integrated flux values measure the rate at which interstitials are supplied to this region. In analogy to the vacancy-induced loss, we assume: (1) the lost interstitials in the loops are due solely to the interstitial undersaturation in the near-surface region; and (2) negligible I–V recombination. With assumption (1), it would appear at first glance that one could measure a  $C_I/C_I^*$  value in direct analogy to the measurement of  $C_V/C_V^*$ . Nevertheless, we cannot measure a  $C_I/C_I^*$  value because we do not know the relative strength

of surface recombination versus the ability of the loops to supply interstitials. While the interface attempts to maintain a value of  $C_I^S$ , the loops attempt to supply interstitials to achieve equilibrium,  $C_I^*$ . The actual value of  $C_I$  at the interface is therefore some concentration  $C_I^{SS}$ , where  $C_I \leq C_I^{SS} \leq C_I^*$ . Figure 8(b) shows a schematic of interstitial concentration with depth, and captures the difficulty in measuring a true  $C_I/C_I^*$  in this system by the method of dislocation loops. Even if we assume a flat profile for the interstitial concentration in the near-surface region, we cannot derive a value for  $C_I/C_I^*$  because  $C_I^{SS}$  is unknown.

Through two indirect observations we conclude that interstitial undersaturation-induced loop dissolution can be disregarded. The number of interstitials bound by the loops is approximately constant, even with a rise in temperature from 810 to 910 °C, indicating the loops are not supplying a significant amount of interstitials to account for the increase in  $C_I^*$ . The estimate by Tan and Gösele<sup>6</sup> yields  $C_I^*(810\text{ °C}) \sim 1.7 \times 10^{10}\text{ cm}^{-3}$  and  $C_I^*(910\text{ °C}) \sim 9.0 \times 10^{11}\text{ cm}^{-3}$ . This substantial increase must instead be supplied by surface or bulk processes. We can make an estimate of the magnitude of interstitial undersaturation-induced loop dissolution from the values of loop growth in an interstitial supersaturation. We noted that by using doping superlattices, a previous study measured  $C_I/C_I^* \sim 0.2$  in Si annealed in  $\text{NH}_3$  at 910 °C.<sup>5</sup> A previous report studied the growth of extrinsic dislocation loops in Si during dry oxidation of the surface.<sup>12</sup> Oxidation of Si results in a supersaturation of interstitials. The relative supersaturation was estimated to be  $C_I/C_I^* \sim 10$ . With 1000% more interstitials present than at equilibrium, the number of interstitials bound by the loops increased by 60%, from  $3.5$  to  $5.5 \times 10^{14}\text{ cm}^{-2}$ , after 60 min at 900 °C. Given the relative magnitude of these values, we would therefore expect that a depletion of 80% of the original interstitial concentration to contribute little to the measured loop dissolution.

#### IV. CONCLUSION

Anneal in  $\text{NH}_3$  of Si that has a preexisting layer of extrinsic dislocation loops from ion implantation results in en-

hanced dissolution of the loops compared to samples annealed in Ar. This enhanced dissolution is due to vacancy supersaturation, with vacancies recombining with interstitials bound by the loops. The decreasing amount of interstitials bound by the loops in the samples annealed in  $\text{NH}_3$  retards coarsening of the loops. We extract values of  $C_V/C_V^* \sim 4$  for annealing Si in  $\text{NH}_3$  at 910 °C. This shows excellent agreement with a previous estimate of vacancy supersaturation measured by antimony dopant diffusion in dopant superlattices.

#### ACKNOWLEDGMENTS

The work at the University of Florida was funded by SEMATECH and the work at Cornell University was funded by the SRC Microstructures Program (Grant No. 95-SC-069). We thank Bell Laboratories, Lucent Technologies for partial financial support of two of the authors (S.B.H. and T.K.M.).

- <sup>1</sup>P. M. Fahey, P. B. Griffin, and J. D. Plummer, *Rev. Mod. Phys.* **61**, 289 (1989).
- <sup>2</sup>K. S. Jones, S. Prussin, and E. R. Weber, *Appl. Phys. A* **45**, 1 (1988).
- <sup>3</sup>P. Fahey, G. Barbuscia, M. Moslehi, and R. W. Dutton, *Appl. Phys. Lett.* **46**, 784 (1985).
- <sup>4</sup>S. T. Ahn, H. W. Kennel, J. D. Plummer, and W. A. Tiller, *Appl. Phys. Lett.* **53**, 1594 (1988).
- <sup>5</sup>T. K. Mogi, H.-J. Gossmann, D. J. Eaglesham, C. J. Rafferty, H. S. Luftman, F. C. Unterwald, T. Boone, J. M. Poate, and M. O. Thompson, in *Proceedings of the Fifth International Symposium on Ultra Large Scale Integration Science and Technology*, edited by Edward Middlesworth and Hisham Massoud (The Electrochemical Society, Pennington, NJ, 1995), p. 145.
- <sup>6</sup>T. Y. Tan and U. Gösele, *Appl. Phys. A* **37**, 1 (1985).
- <sup>7</sup>H.-J. Gossmann, G. H. Gilmer, C. S. Rafferty, F. C. Unterwald, T. Boone, J. M. Poate, H. S. Luftman, and W. Frank, *J. Appl. Phys.* **77**, 1948 (1995).
- <sup>8</sup>J. K. Listebarger, K. S. Jones, and J. A. Slinkman, *J. Appl. Phys.* **73**, 4815 (1993).
- <sup>9</sup>M. M. Moslehi and K. C. Sarawat, *IEEE Trans. Electron Devices* **ED-32**, 106 (1985).
- <sup>10</sup>B. L. Eyre and D. M. Maher, *Philos. Mag.* **24**, 767 (1971).
- <sup>11</sup>H.-J. Gossmann, C. S. Rafferty, P. A. Stolk, D. J. Eaglesham, G. H. Gilmer, J. M. Poate, H.-H. Voung, T. K. Mogi, and M. O. Thompson, *Mater. Res. Soc. Symp. Proc.* **389**, 3 (1995).
- <sup>12</sup>H. Park, K. S. Jones, and M. E. Law, *J. Electrochem. Soc.* **141**, 759 (1994).